# Ground calibrations of Nuclear Compton Telescope

Jeng-Lun Chiu*[a], Zong-Kai Liu[b], Mark S. Bandstra[c], Eric C. Bellm[c], Jau-Shian Liang[a],
Daniel Perez-Becker[c], Andreas Zoglauer[c], Steven E. Boggs[c], Hsiang-Kuang[a] Chang,
Yuan-Hann Chang[b], Minghuey A. Huang[d], Mark Amman[e], Shiuan-Juang Chiang[d], Wei-Che Hung[b],
Chih-Hsun Lin[f], Paul N. Luke[e], Ray-Shine Run[d], and Cornelia B. Wunderer[g]

[a]National Tsing Hua University, Hsinchu City, Taiwan 30013;
[b]National Central University, Taoyuan County, Taiwan 32001;
[c]Space Sciences Laboratory, University of California, Berkeley, CA, USA 94720;
[d]National United University, Miaoli County 36003, Taiwan 36003;
[e]Lawrence Berkeley National Laboratory, Berkeley, CA, USA 94720;
[f]Institute of Physics, Academia Sinica, Taipei, Taiwan 11529;
[g]Detector Group, DESY Photon Science, Hamburg, Germany 22607

## ABSTRACT

The Nuclear Compton Telescope (NCT) is a balloon-borne soft gamma ray (0.2-10 MeV) telescope designed to study astrophysical sources of nuclear line emission and polarization. The heart of NCT is an array of 12 cross-strip germanium detectors, designed to provide 3D positions for each photon interaction with full 3D position resolution to < 2 mm^3. Tracking individual interactions enables Compton imaging, effectively reduces background, and enables the measurement of polarization. The keys to Compton imaging with NCT's detectors are determining the energy deposited in the detector at each strip and tracking the gamma-ray photon interaction within the detector. The 3D positions are provided by the orthogonal X and Y strips, and by determining the interaction depth using the charge collection time difference (CTD) between the anode and cathode. Calibrations of the energy as well as the 3D position of interactions have been completed, and extensive calibration campaigns for the whole system were also conducted using radioactive sources prior to our flights from Ft. Sumner, New Mexico, USA in Spring 2009, and from Alice Springs, Australia in Spring 2010. Here we will present the techniques and results of our ground calibrations so far, and then compare the calibration results of the effective area throughout NCT's field of view with Monte Carlo simulations using a detailed mass model.

Keywords: Gamma-ray astronomy detectors, gamma-ray imaging, Compton imaging, germanium radiation detectors

## 1. INTRODUCTION

The Nuclear Compton Telescope (NCT) is a balloon-borne soft gamma-ray (0.2 to 10 MeV) telescope designed to study astrophysical sources of nuclear line emission and polarization[1-3]. The heart of NCT is an array of 12 cross-strip germanium detectors (GeDs) (Fig. 1 left), designed to provide 3D positions for tracking each photon interaction with full 3D position resolution to 1.6 mm3. Each of the NCT detectors is a 37 x 37 cross-strip planar detector, 15 mm thick. Orthogonal strips are deposited on both faces of the GeD, with a strip pitch of 2 mm, and a 0.25 mm gap between the strips. The entire set of detectors and their cryostat are enclosed inside an active BGO well (Fig. 2), giving an overall field of view of 3.2 sr. The instrument is mounted in a pointed, autonomous balloon platform (gondola).

The NCT instrument was successfully launched from Fort Sumner, New Mexico on May 17, 2009. This flight[4], whose main target was the Crab Nebula/Pulsar, lasted for ~38.5 hours before impacting the ground in the end. Nine of the ten detectors were operational for a total of 22 hours at about 35 km to 40 km altitude. However, in Spring 2010, there was a launch accident occurred to result in major payload damage with no balloon flight, where a subsequent one with the same detector array and gondola was expected from Australia mainly to observe the Galactic Center Region.
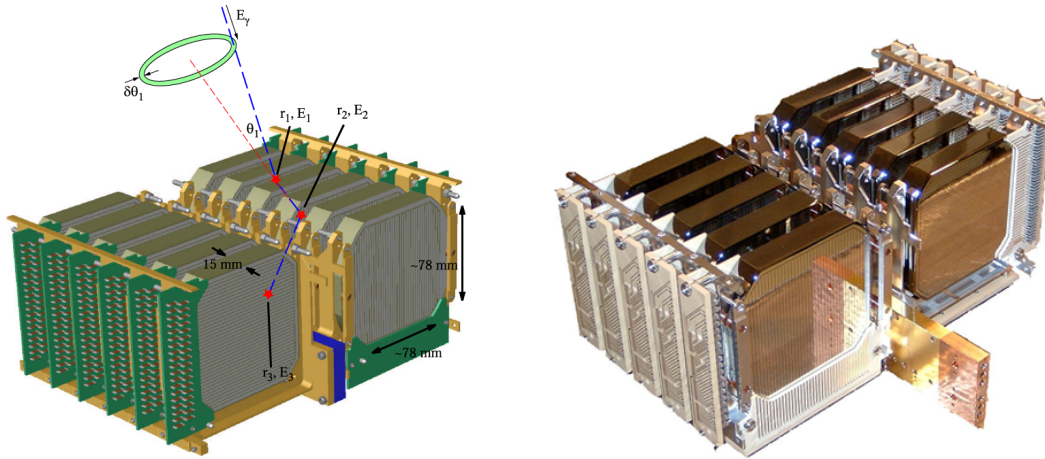
Figure 1. Left: The NCT utilizes 12 cross-strip GeDs with 3D position resolution, excellent spectroscopy, sensitivity to γ-ray polarization, and high efficiency. Right: The 10 germanium cross-strip detectors of NCT that were adopted in the 2009 and 2010 balloon campaigns.
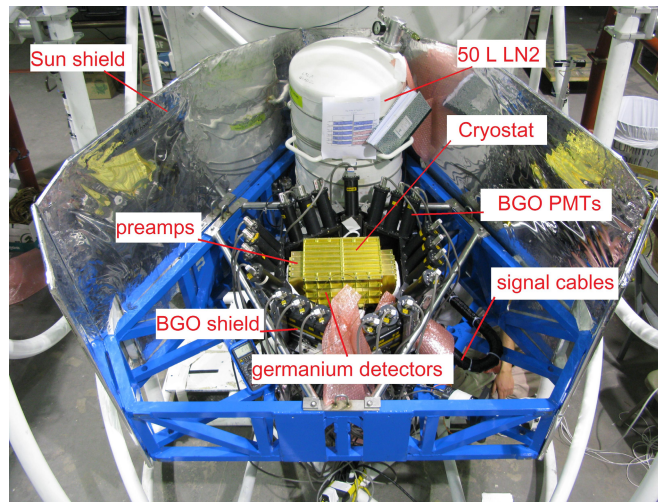


Figure 2. The configuration of NCT instrument in the cradle. The cradle is mounted in a pointed, autonomous balloon platform (gondola).

Data analysis for the flight as well as ground calibrations[5-6] is ongoing against improving data-processing pipeline. In this article, we will focus on the calibration data from 2009 campaign, and extend to those from 2010 in the near future.

The analysis tool adopted for this work is MEGAlib[7], which is a software suite for: (i) data analysis of gamma-ray telescopes, (ii) event and image reconstruction, performance characterization, and (iii) interfacing with Monte Carlo simulation packages GEANT4[8] and MGGPOD[9].

## 2. ENERGY CALIBRATION

The 10-GeD version of NCT flown in 2009 offers several new calibration challenges to overcome. For the energy calibration, the "toaster" configuration (Fig. 1 right) makes illumination of most detectors from normal incidence impossible. Care must be taken to obtain enough counts in each channel of each detector, especially at low energies where photons might not reach shaded portions of some detectors.

The solution has been to take data with the low energy sources placed above each of the gaps between detectors.
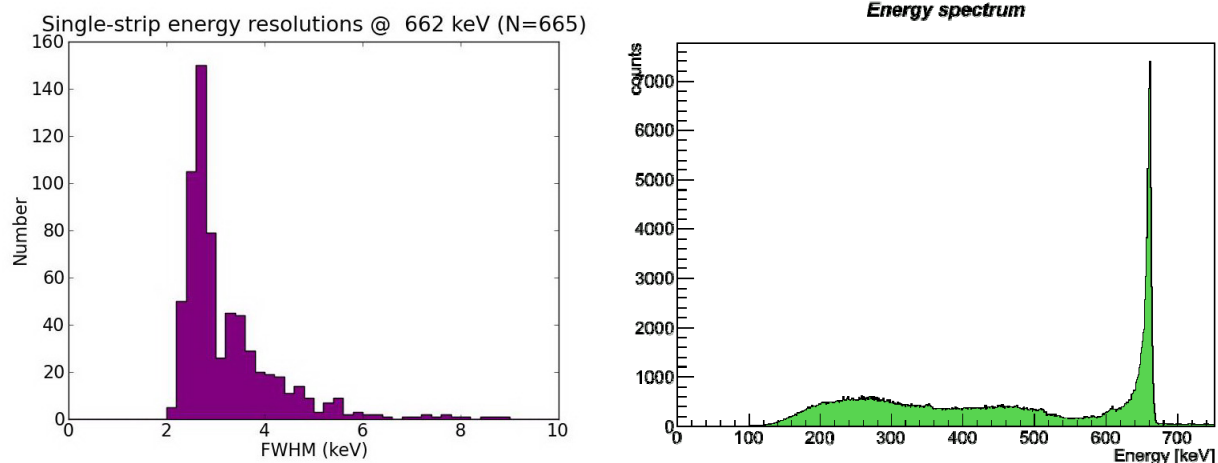
Figure 3. Left: Histogram of single-strip energy resolutions at 662 keV. Right: Spectrum of fully-reconstructed Compton events for 662 keV photons.

High energy sources could still be placed farther away, but more accumulation time was needed than on the 2005 flight. In this way, most of the channels have several calibration lines between 30 keV ($^{129}$I) and 1333 keV ($^{60}$Co), allowing for a complete energy calibration at all relevant energies. A histogram of the energy resolutions for each strip at 662 keV ($^{137}$Cs) is shown in Fig. 3 (left), which reveals that most channels have excellent energy resolution (~0.3-0.9% at 662 keV).

The line positions are then usually fitted to an empirical function, such as a linear or quadratic. Since a significant upturn was seen in the energy-channel plots at low energies, we tried functions that had additional exponential-like terms at lower energies (below ~200 keV). Cross-validation[10, 11] was used to select the most robust model for each strip.

Another measure of the energy calibration is the resolution obtained after performing Compton event reconstruction. Reconstruction is performed using the usual NCT analysis pipeline. Compton events are expected to have a lower resolution than single-site events simply because at least two energy deposits are needed to reconstruct such an event. Fig. 3 (right) shows such a spectrum for a 662 keV source. The measured FWHM of the line is 5.9 keV, or 0.89% resolution.

In order to produce the above reconstructed spectrum, further work on the energy calibration was conducted to correct both the cross-talk of events occurring on adjacent strips and charge-loss of single interaction in the gap between two strips. Adjacent-strip events create tailing below the photopeak and a small spurious peak above the photopeak. This has been seen in similar instruments and can be corrected[12, 13]. Therefore, corrections can be achieved, once knowing peak offset in NCT was linear with total energy as well as dependent on how close the adjacent strips are, and then a charge-loss model to calculate charge fractions between adjacent strips can be introduced to those identified charge-loss events.

## 3. DEPTH CALIBRATION

To determine the energy deposited in the detector at each strips and to track the gamma-ray photon interaction within the detector are the keys to Compton imaging with NCT's detectors. The 3D positions are provided by the orthogonal X and Y strips, and by determining the interaction depth, or z-position. We cannot measure the z-position directly, but we can measure the collection time difference (CTD) of the anode and cathode charge signals, which is related to the interaction depth. The timing channel is measured by a 200 ns shaping time bipolar shaper and stamps the waveform when the signal crosses zero (signal changes from positive to negative) with 10 ns time resolution. The CTD is defined by the difference between two zero-crossing times, and has an error of ~14 ns. The task of depth calibration is to determine the correlation between the CTD and the depth of the interaction.
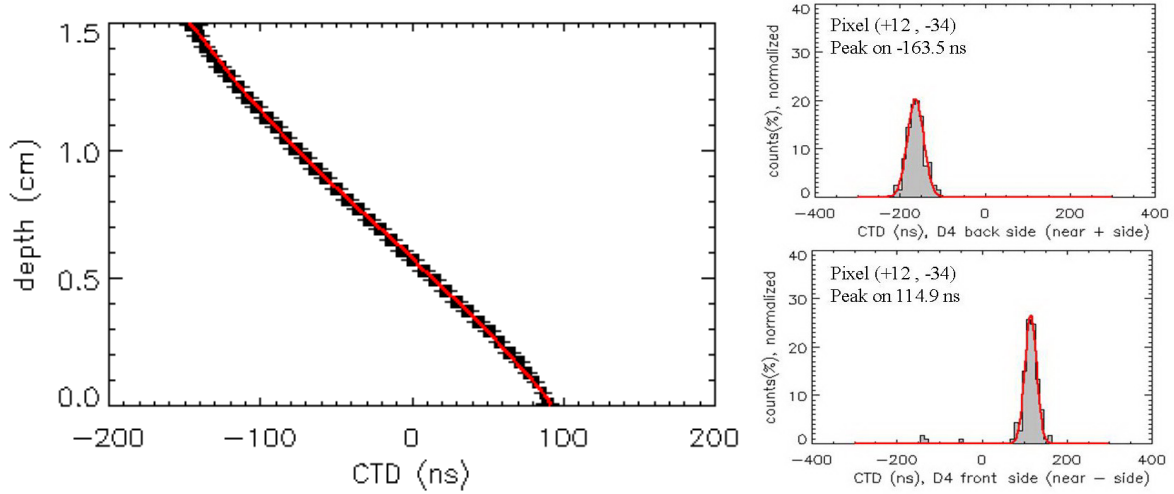
Figure 4. Left: Result of charge transport simulations. The red line is the third-order polynomial fitting. Right: The CTD distribution on both sides of D4. The source we used is $^{241}$Am, where energy line is 60 keV.

The method of depth calibration for NCT prototype is discussed in[14, 15]. We briefly introduce those methods here. The general idea of depth calibration is to find an ideal conversion form for converting CTD to depth, and then to adjust parameters for finding the best form which can fit with data. A custom charge transport simulation model[16] was used for obtaining the ideal form. The relationship between CTD and the depth was assumed to be a cubic polynomial. For only 1 germanium detector, a source was put on one side and only photo peak events were taken for the calibration. Because of the exponential distribution of depth for the photo peak events, one can determine the expected CTD histogram from the ideal depth-CTD conversion form. By fitting the measured data, the best CTD-depth conversion form can be obtained, and the mean free path of the photon also can be determined. One can use the illumination of 60 keV ($^{241}$Am) and 122 keV ($^{57}$Co) sources from both sides of the detector to check the consistence of mean free path from both side of illumination, and also can verify the agreement with both sources.

However, illumination from both sides for each detector becomes difficult for many detectors. Instead of the exponential depth distribution, another known distribution is needed. One can use a simulation tool (e.g. MGEANT[17]) to create a known depth distribution and obtain a template of the CTD from the ideal depth-CTD conversion form. A best CTD-depth conversion form can also be obtained by fitting with calibration data. We use $^{137}$Cs to do the depth calibration for NCT prototype. Since the number of 662 keV photo peak events is small, the continuum events should also be taken into account. A background model is used for the continuum. More details are discussed in [15]. For the NCT'09 depth calibration, we use another method which is described below.

In the previous work, we fit the measured data by tuning two parameters in the assumed linear correlation between the measured CTD ($\tau$) and CTD template ($\tau'$) [15]:

$$\tau = \eta\tau' + \Delta \qquad\qquad (1)$$

The two parameters are the "stretching factor" $\eta$ and "time offset" $\Delta$. The stretching factor $\eta$ accounts for electric field variations in the detector. The time offset $\Delta$ is included to account for electronics channel variations. We also keep this assumption in our work.

The method we used for the depth calibration consists of 4 steps:

(i) Obtain an ideal CTD-depth conversion form by using a custom charge transport simulations model and a bipolar shaping model of NCT's fast channel (Fig. 4 left). The charge transport simulations give the charge signal from the detectors, and the bipolar shaping model simulates the timing response of the NCT electronics.

(ii) Use the $^{241}$Am source (60 keV) to find a CTD distribution near the surface on both sides (Fig. 4 right). The source is put on the top of the gap between two detectors to trigger all the pixels on one side of detector.
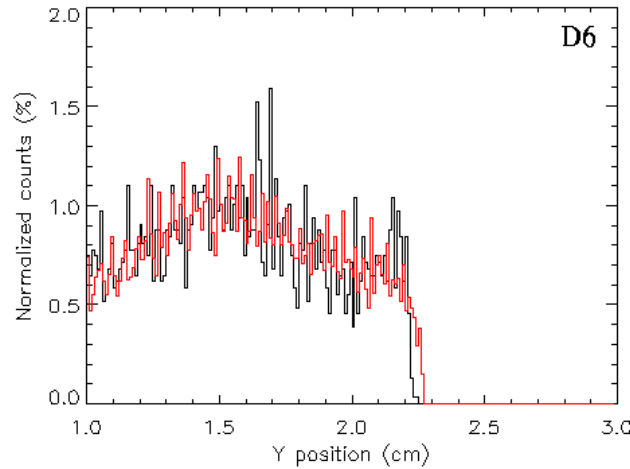
Figure 5. The depth distribution of D6. A $^{137}$Cs source was put on top of the NCT detector. Calibration data (red) are consistent with simulation results (black) except for the edge region. This is because the conversion curve adopted in the simulation can not convert the CTD back to depth perfectly.

(iii) Use MGEANT to obtain the ideal CTD distribution of the $^{241}$Am source on both sides. The ideal CTD-depth conversion form from step one is used here.

(iv) We now have two sets of ideal and measured CTD which are from the step (ii) and (iii). The η and Δ in the assumed linear conversion form between measured CTD (τ) and ideal CTD (τ') can be easily obtained from those two sets of τ and τ'. Once the η and Δ are known, the interaction depth can be determined from the measured CTD by two conversion form of "measured CTD to ideal CTD" and "ideal CTD to depth".

To verify those two forms, one has to take different calibration data and verify the consistency between simulated and measured depth. We checked this depth calibration method by using $^{137}$Cs data. Both simulations and measure-ments went though the same data processing pipeline, called Nuclearizer, and we obtained the depth distribution of the first interaction from MEGAlib. The Nuclearizer is a low level reconstruction tool for NCT, including the detector effect engine module, calibration module and strip pairing module. Figure 5 shows the comparison between simulations and measurements. The difference on the edge is due to the edge effect. Both the cubic polynomial form from the calibration and the detector effect simulation cannot perform well in the edge region. Average position resolutions are estimated to be 0.40 mm to 0.76 mm due to different timing window by using the simulation with a time resolution of 10 ns, and become 0.50 mm to 0.83 mm while including an assumed timing noise of 15 ns FWHM.

## 4. EFFECTIVE AREA CALIBRATION

Instead of completely calibrating our detectors using laboratory measurements against the quite large phase space of photon energies, directions, and interaction sequences present in wide-field Compton imaging, the analysis in NCT employs Monte Carlo simulations using a detailed mass model which are optimized to accurately reproduce the measurements.

Effective-area calibrations as well as verifications of imaging performance were then carried out using radioactive sources and a theodolite (Fig. 6), which enables us to obtain cm-scale localization of the radioactive sources and to make an effective comparison with the measured data. Even though being constrained by the hanger in Fort Sumner, 3.5–6.5 meter source-detector separations we obtained were adequate to test NCT's far-field imaging prior to the balloon flight. Two-hour observations of several sources, which were also designed for efficiency calibrations, were conducted

throughout NCT's field of view. The sources chosen to cover a broad portion of NCT's imaging energy range are: $^{57}$Co (122 keV), $^{133}$Ba (81, 303, and 356 keV), $^{137}$Cs (662 keV), and $^{60}$Co (1.17 and 1.33 MeV). Our precise localizations also



Figure 6. Setup for the effective area calibration. The sources were placed 5 m away from the detectors on the center of an aluminum board (upper left). A theodolite (lower right corner) was adopted to determine the source positions by several sightings on the board and cryostat.

ensure that the dominant contribution to our uncertainty in the calculated effective area is due to the ~ 1.2% (1$\sigma$) uncertainty in the calibrated source activities. In this work, we will present preliminary analysis of the $^{137}$Cs and $^{60}$Co data.

Using MEGAlib, images can be obtained based on certain event selections to allow us to compare the result with our setup. Besides, our group have also developed a "detector effects engine" to convert the precise energy and position information output by the GEANT4 simulations to the strip hits and energy channel data that NCT's detectors return. The engine includes charge sharing, charge loss, and current depth and energy calibrations. Thus, the Compton event reconstruction methods are applied identically to equivalent data from both simulation and calibration.

Figure 7 compares the measured and simulated effective area at several points along the centerline of the NCT field of view. Identical event selections were applied to the simulations and to the data. Only events with total deposited energies within 1.4$\sigma$ of the observed photopeak were included. However, this preliminary analysis does not include spatial cuts on the direction of the incident photon. Our preliminary results show general agreement between the measured and the simulated efficiencies. The largest discrepancies occur for measurements on axis. In this geometry, only the top edge of the NCT GeDs is exposed to incoming photons. Edge field effects in some GeDs have reduced the efficiency of the 2–3 strips closest to the edges. This phenomenon is not yet modeled by our detector effects engine, which may explain the over-prediction of the simulation. It is also possible that our simulations of the veto provided by the guard ring surrounding the GeD could be improved. In general, however, few systematic biases are apparent when comparing the data and simulations, giving credence to our analysis methods. Future work with these calibration data will further improve the correspondence between simulation and measurement. A spatial cut on the direction of the incident photon will help remove background events and poorly reconstructed interactions. Performance will also be improved by further refinements of the low-level energy and depth calibrations as well as our detector effects engine.

Although there was no flight in 2010 campaign, the pre-flight calibrations were still good sources to verify the instrument performance. Comparison with data from 2009 campaign is also expectable, since almost all the system

configuration is the same. Furthermore, new data taken with other radioactive sources, such as [88]Y (0.898 and 1.836 MeV) and [133]Ba (81, 303, and 356 keV) (Fig. 8), will help us to extend our current results to wider phase space.
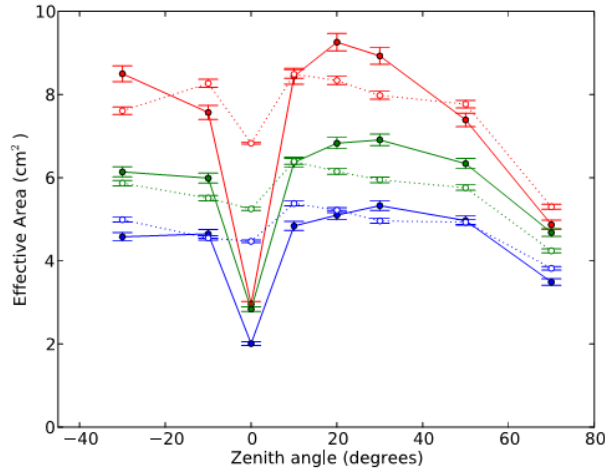


Figure 7. Measured and simulated NCT effective area on axis at 662 keV (red), 1173 keV (green), and 1333 keV (blue). Calibration data have solid lines and points, while simulations have dashed lines and open symbols. Errors are 90% C.L.
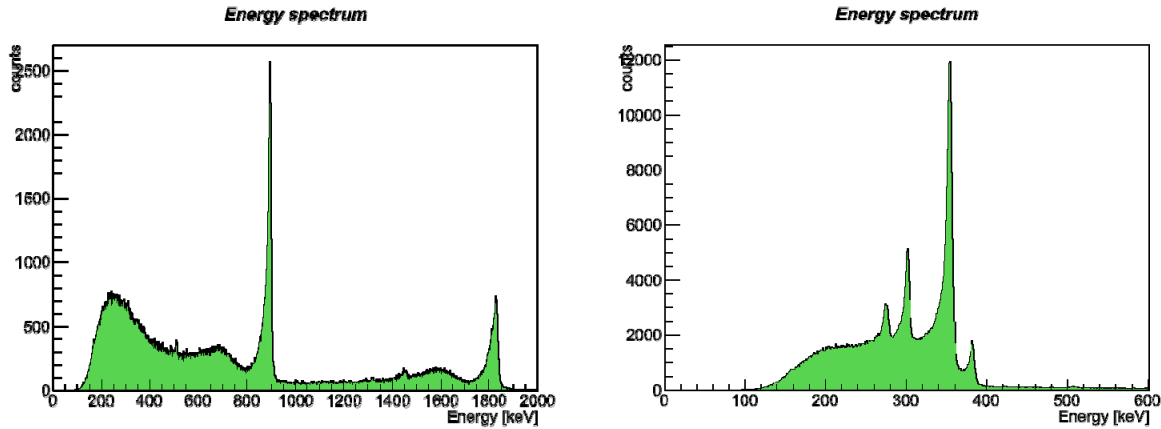


Figure 8. Spectra of two effective-area calibrations obtained from 2010 campaign. Left: [88]Y (0.898 and 1.836 MeV); Right: [133]Ba (81, 303, and 356 keV)  at zenith 20° on-axis.

## 5.  IMAGING CAPABILITY

The configuration of imaging-performance verifications was the same as that in effective-area calibrations. The reconstructed photo peaks (Fig. 11) in one of our calibration data are consistent with the measured source positions (crosses) within 1°. Although the angular resolution for either source here is about 9°, it is still possible to distinguish these two sources in Fig. 9 even when they are about 6° away (i.e. above their half maxima), if there's a good signal-to-noise ratio.

# 6. SUMMARY

We have performed energy calibrations, which achieved average energy resolutions for the different detectors ranging from 1.8-3.0 keV FWHM at 60 keV to 2.7-6.3 keV FWHM at 1333 keV, and the full-reconstructed spectral resolution at 662 keV was about 5.9 keV after cross-talk and charge-loss correction.

A simulation-intensive technique has been developed for calibrating the depth of interactions in our planar germanium cross-strip detectors adequately. Later, these two calibrations will be improved to obtain better performance.
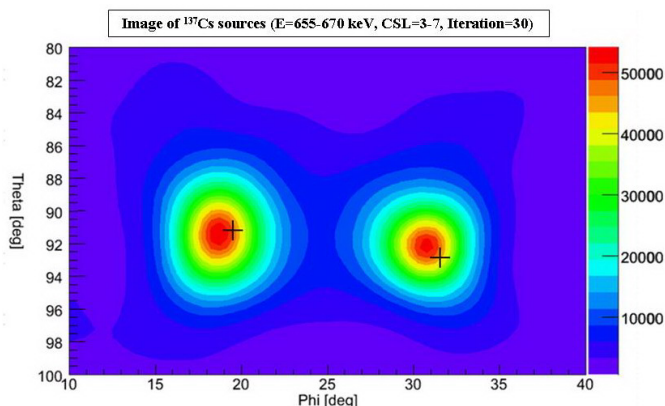


Figure 9. The image with two $^{137}$Cs sources that are ~10° away. Two sets of data from two different positions are included in this image to examine both localization and separation capabilities of imaging. Photons adopted here are 3- to 7- site events inside ~1.4 σ of energy peak (662 keV), and classic expectation-maximization algorithm in 30 iterations was then introduced for further image reconstruction. Crosses indicate the measured source positions by theodolite.

A preliminary analysis of the $^{137}$Cs and $^{60}$Co data for effective-area calibrations was presented, and more work is being processed to compare the real data and simulation.

Imaging capabilities enables us to localize a $^{137}$Cs source within 1° precision and to distinguish $^{137}$Cs sources ~6° away, even though the angular resolution is ~9°. That is, the location accuracy is now much higher than the angular resolution. Some more imaging tests will be carried out to examine the imaging capabilities.

# ACKNOWLEDGEMENT

# REFERENCES

[1] Boggs, S. E., Coburn, W., Smith, D. M., Bowen, J. D., Jean, P., Kregenow, J. M., Lin, R. P., and von Ballmoos, P., "Overview of the Nuclear Compton Telescope," New Astron. Rev. **48**, 251–255 (2004).

[2] Boggs, S., Bandstra, M., Bowen, J., Coburn, W., Lin, R., Wunderer, C., Zoglauer, A., Amman, M., Luke, P., Jean, P., and von Ballmoos, P., "Performance of the Nuclear Compton Telescope," Experimental Astronomy, 25–32 (2006).

[3] Chang, H.-K., Boggs, S., and Chang, Y.-H., "The Nuclear Compton Telescope (NCT): Scientific goals and expected sensitivity," *Advances in Space Research* **40**, 1281–1287 (2007).

[4] Bandstra, M., Bellm, E., Chiu, J.-L., Liang, J.-S., Liu, Z.-K., Perez-Becker, D., Zoglauer, A., Boggs, S., Chang, H.-K., Chang, Y.-H., Huang, M.-H., Amman, M., Chiang, S. J., Hung, W.-C., Jean, P., Lin, C.-H., Luke, P., Run, R.-S.,

and Wunderer, C., "The spring 2009 balloon flight of the nuclear Compton telescope," in [Nuclear Science Symposium Conference Record (NSS/MIC), 2009 IEEE], 2131 –2139 (2009).

[5] Chiu, J.-L., Liu, Z.-K., Bandstra, M., Perez-Becker, D., Bellm, E., Zoglauer, A., Boggs, S., Chang, H.-K., Chang, Y.-H., Huang, M., Amman, M., Hung, W.-C., Liang, J.-S., Lin, C.-H., Luke, P., Run, R.-S., and Wunderer, C., "Energy, depth calibration, and imaging capability of nuclear compton telescope," in [Nuclear Science Symposium Conference Record (NSS/MIC), 2009 IEEE], 472 –476 (2009).

[6] Bellm, E. C., Chiu, J.-L., Perez-Becker, D., Liang, J.-S., Zoglauer, A., Bandstra, M. S., Liu, Z.-K., Boggs, S. E., Chang, H.-K., Chang, Y.-H., Huang, M. A., Amman, M., Hung, W.-C., Jean, P., Lin, C.-H., Luke, P. N., Run, R.-S., and Wunderer, C. B., "Efficiency and polarimetric calibration of the nuclear compton telescope," in [Nuclear Science Symposium Conference Record (NSS/MIC), 2009 IEEE], 444 –448 (2009).

[7] Zoglauer, A., Andritschke, R., and Schopper, F., "MEGAlib — The Medium Energy Gamma-Ray Astronomy Library," New Astron. Rev. **50**, 629–632 (2006).

[8] Agostinelli, S. et al., "GEANT4 - a simulation toolkit", Nuclear Instruments and Methods in Physics Research Section A **506**, 250-303 (2003).

[9] Weidenspointner, G., Harris, M. J., Sturner, S., Teegarden, B. J., and Ferguson, C., "MGGPOD: a Monte Carlo Suite for Modeling Instrumental Line and Continuum Backgrounds in Gamma-Ray Astronomy," Astrophys. J., Suppl. Ser. **156**, 69–91 (2005).

[10] Stone, M., "Cross-validatory choice and assessment of statistical predic-ations," Journal of the Royal Statistical Society. Series B **3**, 111–147 (1974).

[11] Geisser, S., "The predictive sample reuse method with applications," Journal of the American Statistical Association **70**, 320–328 (1975).

[12] Cooper, R. J., Boston, A. J., Boston, H. C., Cresswell, J. R., Grint, A. N., Harkness, L. J., Nolan, P. J., Oxley, D. C., Scraggs, D. P., Lazarus, I., Simpson, J., and Dobson, J., "Charge collection performance of a segmented planar high-purity germanium detector," Nuclear Instruments and Methods in Physics Research Section A **595**, 401-409 (2008).

[13] Gros, S., Hammond, N. J., Lister, C. J., Chowdhury, P., Fischer, S. M., and Freeman, S. J., "Performance tests of large area position-sensitive planar germanium detectors with conventional and amorphous contacts," Nuclear Instruments and Methods in Physics Research Section A **602**, 467-476 (2009).

[14] Amrose, S., Boggs, S. E., Coburn, W., Lin, R. P., and Smith, D. M., "Calibration of 3D position in a Ge cross-strip detector," Nucl. Instrum. Meth. Phys. Res. A **505**, 170–173 (2003).

[15] Bandstra, M., Bowen, J., Zoglauer, A., Boggs, S., Coburn, W., Wunderer, C., Amman, M., and Luke, P., "Position calibrations and preliminary angular resolution of the prototype nuclear compton telescope," in [Nuclear Science Symposium Conference Record, 2006. IEEE], 2, 770 –777 (2006).

[16] Amrose, S., Boggs, S. E., Coburn, W., Holland, G., Lin, R. P., and Smith, D. M., "Numerical simulations of 3D positioning in cross-strip Ge detector," in Proc. Nucl. Sci. Symp. Conf. Rec. **1**, 230–233. (2001).

[17] Sturner, S. J., Seifert, H., Shrader, C., and Teegarden, B.J., "MGEANT - A GEANT-based multi-purpose simulation package for gamma-ray astronomy missions," Proc. AIP Conf. **510**, 814-818 (2000).